A GIS-BASED PROCEDURE FOR MEASURING THE EFFECTS OF THE BUILT ENVIRONMENT ON URBAN FLASH FLOODS

Yan Li[1] and Chunlu Liu[2]

ABSTRACT

Urban flooding has been a severe problem for many cities around the world as it remains one of the greatest threats to the property and safety of human communities. In Australia, it is seen as the most expensive natural hazard. However, urban areas that are impervious to rainwater have been sharply increasing owing to booming construction activities and rapid urbanisation. The change in the built environment may cause more frequent and longer duration of flooding in flood-prone urban regions. Thus, the flood inundation issue associated with the effects of land uses needs to be explored and developed. This research constructs a framework for modelling urban flood inundation. Different rainfall events are then designed for examining the impact on flash floods generated by land-use changes. Measurement is formulated for changes of topographical features over a real time series. Geographic Information System (GIS) technologies are then utilised to visualise the effects of land-use changes on flood inundation under different types of storms. Based on a community-based case study, the results reveal that the built environment leads to varying degrees of aggravation of urban flash floods with different storm events and a few rainwater storage units may slightly mitigate flooding extents under different storm conditions. Hence, it is recommended that the outcomes of this study could be applied to flood assessment measures for urban development and the attained results could be utilised in government planning to raise awareness of flood hazard.

KEYWORDS

land use; GIS; Numerical simulation; Facility construction; Stormwater management

1. INTRODUCTION

Urban flooding has been a severe problem for many cities around the world as it remains one of the greatest threats to the property and safety of human communities (Jha et al., 2012). It ranges from minor incidents, such as flooding of some low-lying areas, to major ones, where

1. School of Architecture and Built Environment, Deakin University, Geelong Australia
2. School of Architecture and Built Environment, Deakin University, Geelong Australia, chunlu@deakin.edu.au (corresponding author)

flooding of extensive urban areas causes economic damage and loss of human life (Mark et al., 2004). Although rapid urbanisation has led to an increase in economic and social wealth in many regions, this development greatly impacts the water sustainability in the built environment (Lee and Heaney, 2003). There may be an unwanted side effect on flood inundation in flood-prone urban areas due to this process (Sheng and Wilson, 2009).

Over the last four decades, flooding events have resulted in personal injury and death in Australia and have cost the economy hundreds of millions. For example, severe flash flooding induced by storms resulted in heavy damage to Sydney's suburbs in April 1974 and March 1975. The total damage cost A$98 million and A$63 million, respectively (Australian Government Bureau of Meteorology (BOM), 2015a). Moreover, a state-wide flood hit Australian Queensland between December 2010 and January 2011, leading to A$2.38 billion in economic damage (Carbone and Hanson, 2013) and A$40 billion reduction in Australia's GDP (ABC News, 2011). More recently, a severe thunderstorm that drenched Victoria's second largest city, Geelong, on 19 February 2014, was recorded with 54mm of rainfall in an hour at the Geelong Racecourse. The ponding water rose to waist height in low-lying areas due to drainage systems being blocked by rainwater (Mills, 2014). Flood inundation has been seen as the most expensive natural hazard in Australia because of an estimated annual cost of more than A$377 million (Middelmann, 2009).

2. BACKGROUND

2.1. Effects of Built Environment

According to the categorisation of flooding events, flash floods result from relatively short, intense bursts of rainfall, often from severe thunderstorms, when urban drainage networks do not have the capacity to convey the excess rainwater (BOM, 2013). In addition, there are several significant factors influencing the storm-induced urban floods such as urban terrain and drainage capabilities. For example, depressions are more prone to flash flooding (Youssef et al., 2011).

Flash flooding is closely related to land management strategies and urban infrastructure construction. Yet there has been ongoing expansion of urbanised areas for many cities around the world. A major component of urbanisation and contributor to flood occurrence is the increase in impervious surfaces (Brody et al., 2008). The impervious ground surface area is increasing with rapid urban development, which means more frequent and longer duration of flooding in flood-prone urban regions due to the increase in rainfall-runoff volumes and flow velocities (Wu et al., 2012). In other words, it is possible that rapid urbanisation increases the risk of flooding and resultant damage. In addition, the relationship between urbanised areas and flash floods relies not only on the amount of impervious ground surface, but specifically where in the hydrological landscape that surface is located (Brody et al., 2014). For example, urban areas are more likely to be flooded than surrounding areas that are not urbanised (National Oceanic and Atmospheric Administration, 2010). Thus, sustainable urban development aids in reducing the risk of flooding and harm to life and community infrastructure, as well as significantly protecting the built environment. However, the effects of land-use changes on flash floods should be evaluated prior to development. An important step in measuring the effects is to appropriately model urban flooding for the identification of vulnerable areas and the prediction of ponding extents.

2.2. Urban Inundation Related Models

Flash floods are predictable based on hydrological models. This means that modelling and measuring urban flood inundation should be explored and developed for reducing flooding damage during development periods. Extensive research has been conducted into storm-induced floods and several feasible methods have been presented in recent years. Among previous paradigms, the American Society of Civil Engineers (1993) compared two common flooding models, namely a 1D sewer model coupled with a 1D surface network and a 1D sewer model coupled with 2D surface flow. The authors indicated that the 1D/1D model can provide a satisfactory approximation with low computational cost. The 1D/2D approach can effectively model complex overland flow according to real urban terrain. Prior to that, Yen and Chow (1980) employed an urban inundation model through combining the Storm Water Management Model (SWMM) with a 2D diffusive overland-flow model, simulating flood inundation as a result of the overflow of rainwater from urban drainage systems. Although the 1D hydrodynamic model was also utilised to simulate urban flooding and proposed flood inundation maps in a Geographic Information System (GIS) environment, results revealed that this 1D model was insufficient to compute flow paths over complex surfaces with dense buildings and infrastructure (Mark et al., 2004). In 2009, the SWMM was also adopted by Dongquan et al. (2009) for an experimental catchment in Macau. The algorithm adopted an automatic batch process with a highly efficient model construction in order to delineate catchments and compute key parameters. More recently, Quan (2014) presented an assessment for rainstorm waterlogging risks in central urban areas of Shanghai, and proposed the ponding distribution and water depth simulation through a simplified urban waterlogging model that combines a SCS model with GIS spatial analysis.

In addition, a spatially-weighted linear regression model was used to conduct observational and empirical research for the impact of land-use characteristics (Brody et al., 2014). There is, however, a lack of hydrological models for measuring the impacts of the built environment on possible flash floods. A GIS-based approach integrating topographical and land-use datasets was developed by Dawod et al. (2011) for investigating the effects from catchment areas and basin stream length in Makkah metropolitan areas. Nevertheless, little research has explored the flood inundation issue based on the land-use change over a real time series. With the rapid development of urbanised regions, soil features have frequently changed over past years. This study aims to examine impacts on flash floods on the basis of changes of topographical features including building and road construction. To more accurately reflect the spatial variation from construction activities, the approach constructs a rain-runoff model based on a catchment mesh. GIS mapping technologies are then used to visualise the land-use effects on flood inundation after simulation.

3. A METHOD FOR MEASURING LAND-USE EFFECTS

In order to examine the effects, an urban flood inundation program should be systematically designed based on urban terrain, surface runoff and drainage systems. Urban terrain indicates the urban environment, determining flow direction and accumulation. A digital elevation model (DEM) is capable of estimating flooding status on the ground surfaces as it could provide sufficient information to describe the continuously varying topographic surfaces. In addition, the DEM, derived mainly from contour data form topographic maps, is a digital representation of a terrain's surface with latitude, longitude and elevation (Thomas et al.,

2015). It can be produced with ArcGIS software based on dense spot elevations and revised according to real topographical features like buildings and roads.

Surface runoff is the rainwater that flows over the land surface, derived mainly from rainfall-runoff and sewer surcharge. According to the water balance theory (Chen et al., 2009) formulated as Equation (1), the amount of surface runoff (Q^r) can be expressed using the total precipitation volume (Q^p), the amount of infiltration (Q^f), the amount of evaporation (Q^e) and the amount of drainage water (Q^d). For a single rainfall event, evaporation can be negligible because of the minute amount in a short time (Mark et al., 2001).

$$Q^r = Q^p - Q^f - Q^e - Q^d \tag{1}$$

Precipitation volume can be defined in terms of rainfall intensity and duration. Rainfall intensity I indicates the ratio of the total amount of the rain falling during a given period to the duration of the period, expressed in depth units per unit time (Pazwash, 2011). The time distribution of precipitation can be specified using several methods such as the alternating block (AB) method (Chow et al., 1988) and the triangular hyetograph (TH) method (Yen and Chow, 1980).

For given land uses and soil types, the Soil Conservation Service curve number (SCS-CN) approach can be used to measure the extent to which a rainstorm penetrates the ground and the amount of runoff that a rainstorm produces during a single storm event. the SCS-CN approach proposed by US Soil Conservation Service (1986) is considered the most popular because of its simplicity and suitability (Jiao et al., 2015), and it has been widely applied in hydrology and environmental studies around the world (Nagarajan and Poongothai, 2012; Zhang and Pan, 2014; Mishra and Singh, 2003; Ranjan et al., 2009). In addition, the SCS-CN method can be integrated with GIS tools for enhancing the accuracy and precision of runoff prediction (Kadam et al., 2012). A fundamental assumption is that the ratio of direct runoff to effective rainfall equals the ratio of actual penetration to potential maximum soil moisture retention S. The other assumption is that the initial abstraction is equal to the product of the initial abstraction coefficient λ and the potential maximum retention (Soulis et al., 2009). Thus, the 1D runoff R in depth can be expressed as:

$$R = (P - \lambda \cdot S)^2 / [P + (1 - \lambda) \cdot S] \tag{2}$$

R is equal to zero if precipitation P in depth is less than 0.2S. In addition, λ is set as 0.05 (Woodward et al., 2003) and S is equal to $25400/CN$-254 with curve number (CN) values varying from 0 to 100.

A distributed model often requires spatial variation. Thus, a catchment mesh is introduced into this study and used to discretise the map so that the model can more accurately calculate regional rainfall-runoff volumes and drainage capabilities within a given study area. Furthermore, the catchment delineation depends on topographical and drainage network data (Mark et al., 2004). It can be presented by the Thiessen polygon method (Thiessen, 1911). The runoff volume over the mth catchment can be expressed as

$$Q_m^p - Q_m^f = \sum_{n=1}^{N} A_n R_n \tag{3}$$

where n denotes the nth type land, such as grassland, carpark or building land. A_n means the projected area of the nth type land on the mth catchment.

The urban drainage model aims to simulate underground drainage pipe networks and to run flow computations. So far, several hydrological models have been explored and developed, such as the SWMM (Rossman, 2010), Infoworks-CS (Wallingford Software, 2006) and the Modelling of Urban Sewers (MOUSE) (Danish Hydraulic Institute, 1999). SWMM was first developed in 1971 for mainframe computers. The latest re-write of SWMM provided by the U.S. Environmental Protection Agency allows the simulation of runoff quantity and quality, as well as polluting loads through a combined sewer system (Rossman, 2010). MOUSE is an advanced modelling package that provides a hydrodynamic pipe flow model through simulation of the water flow of a drainage system (Kubý and Gustafsson, 2001). As a dynamic model for sewer system analysis, MOUSE includes a scheme to solve for hydraulic balance and continuity at each time step. Since the appropriate hydraulic description can be chosen in the pipe module, its pipe flow model engine can efficiently analyse drainage network performance (Smart and Herbertson, 1992). Therefore, MOUSE is employed in this research.

4. CASE STUDY

For the preliminary application of the proposed method, this research considers the Geelong Waurn Ponds (WP) Campus of Deakin University as a community-based study area. Due to much change of topographical features over the last decade, this area represents a typical case study for measuring the impacts on flood inundation from facility construction. As shown in

FIGURE 1. Location and current topographical features of WP campus.

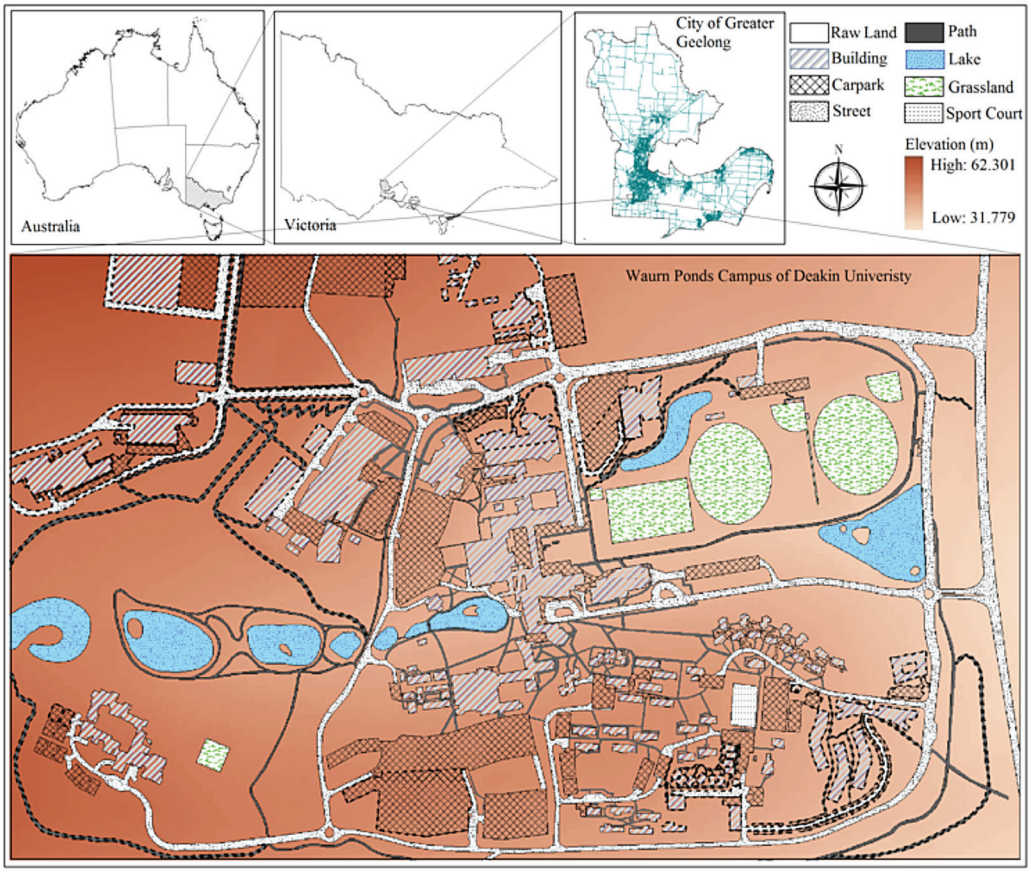

Figure 1, the WP campus (38.1979° S, 144.2973° E) is situated in the south of the City of Greater Geelong, and this study area covers an area of around 1.14 km^2. In order to describe terrain surfaces of this area, the background of the WP campus map displays a high resolution DEM raster with 2 m × 2 m cell size, in which higher elevations are shown in darker colours.

In addition, the WP campus provides various community facilities including a library, office buildings, student residences and sporting fields. The current infrastructure layout and land uses on January 2015 (Jan15) are shown in Figure 1. Land uses are grouped into 8 land types as exhibited in the legend. The previous infrastructure layout and land uses on July 2004 (Jul04) are depicted in Figure 2. In order to clearly differentiate between these two layouts and compare the construction-induced change in the built environment, the structures and infrastructure built between the two periods are outlined by dotted lines, as shown in the Jan15 layout of Figure 1.

FIGURE 2. Previous topographical features and drainage system of WP campus.

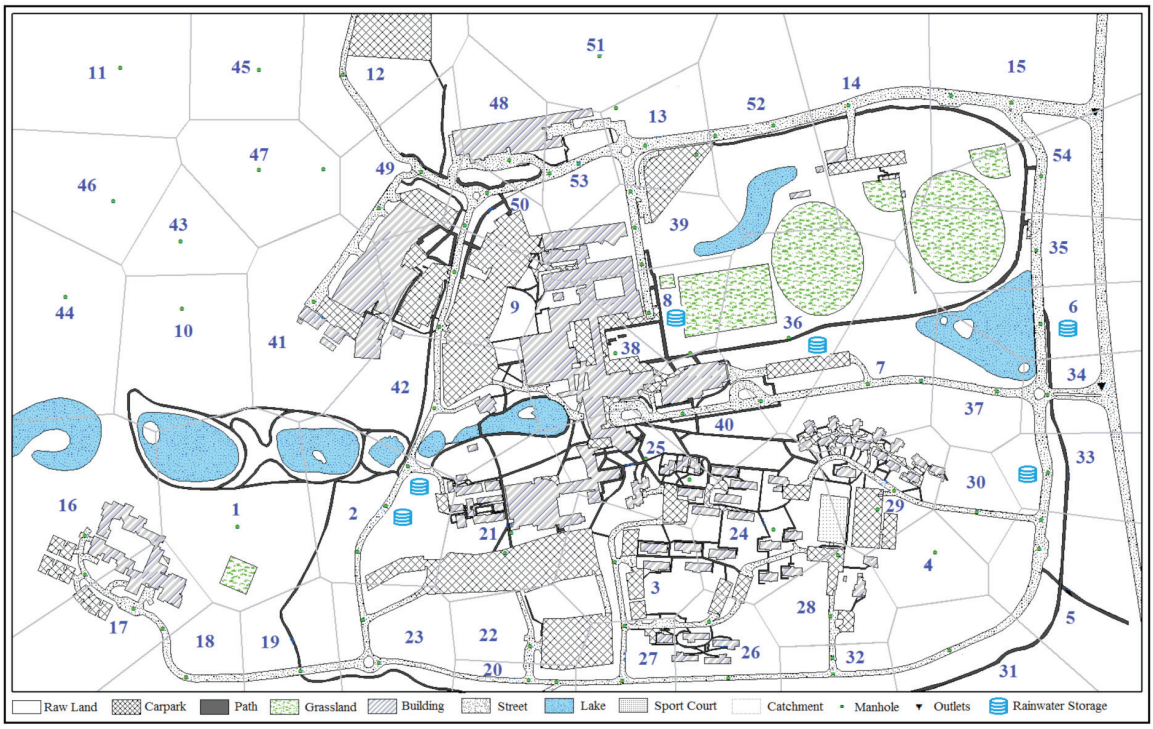

Rainfall intensities can be estimated through reading local intensity-duration-frequency curves (See Figure 3), which are based on the longitude and latitude of the WP campus and rain return periods.

If a rainfall event with an average recurrence interval of 50 years is employed in this research, the AB method can be then employed to generate a rainstorm (Storm AB) by specifying the temporal distribution of rainfall intensities. As shown in Figure 4, the total rain depth can reach 100.26mm, which is very close to the highest daily rainfall record. The nearest rain station to the WP campus recorded that the two highest daily rainfall volumes between 1983 and 2011 were 100mm on 27 January 2005 and 98.8mm on 3 February 2005 (BOM, 2015b). As the temporal distribution varies according to different rainfall types, the

FIGURE 3. Rainfall intensity chart (BOM, 2015c)

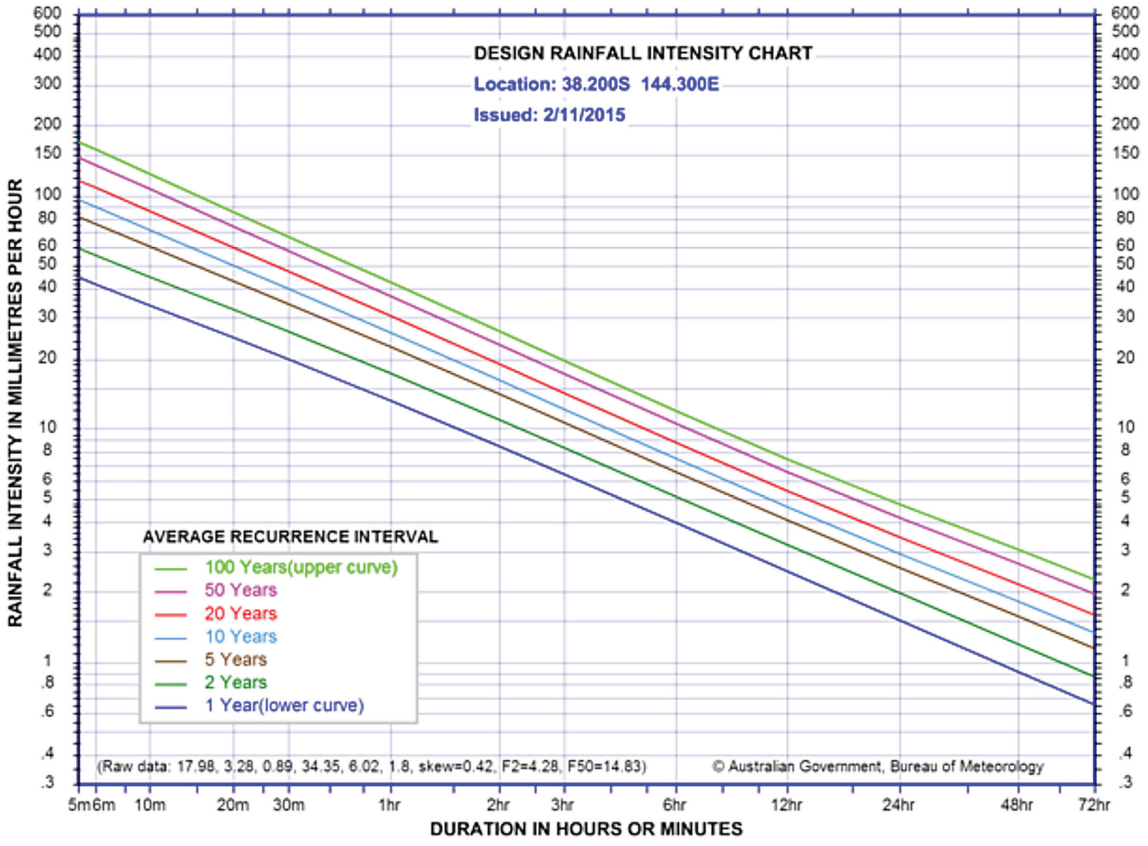

FIGURE 4. Rainstorm hyetograph

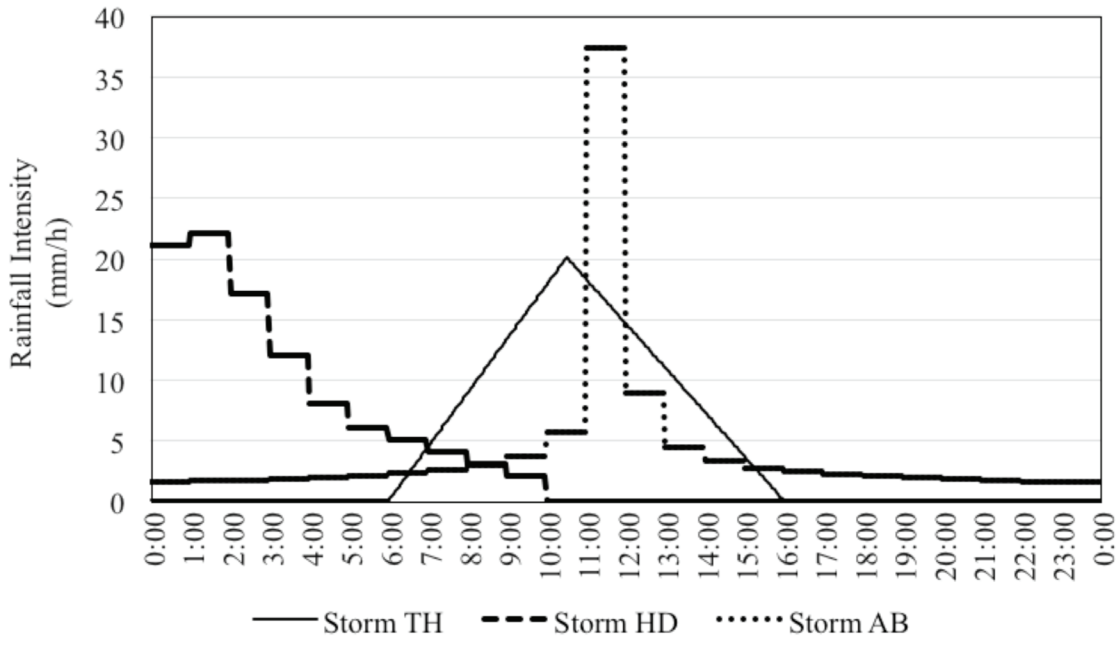

TH method is also adopted to produce Storm TH for simulating another rain scenario (See Figure 4). Its total rain depth is still set as 100.26mm, but its rainfall duration is shortened to 10 hours. Another temporal distribution similar to a Type I Huff Distribution (Huff, 1967) is also proposed as the scenario, Storm HD. Its rainfall depth and duration are also defined as 100.26mm and 10 hours respectively, but the peak rainfall is in the early part of its rainfall distribution and the rainfall intensity gradually decreases like a common rainfall event. These three hypothetical precipitations have peak rainfall intensities of 20.05 mm/h, 22.06 mm/h and 37.34 mm/h, respectively. Moreover, the rainfall loads are here assumed to be uniformly distributed over the study area as the campus is not large enough to take into account the spatial variation of rainfall volumes.

Based on the SCS-CN method, soils are classified into different hydrological groups in terms of infiltration and classification, so that the corresponding CN values can be selected from tables for the land cover conditions. In this research, the CN values are set for raw land at 80, building land at 98, car parks at 98, roads at 98, paths at 92, water bodies at 100, grassland at 75 and sports grounds at 90, based on the TR-55 manual (US Soil Conservation Service, 1986). In addition, 54 rainfall-runoff catchments that are presented in Figure 2 are used to discretise the WP map in the terms of main manholes. MOUSE is employed in this research for simplified drainage systems, which has been proposed based on field observations. Figure 2 depicts the main manholes and two outlets connected with external drainage systems. This drainage network is assumed to operate with a full capacity in the initial conditions.

5. EVALUATION AND DISCUSSION OF CONSTRUCTION-INDUCED EFFECTS

5.1. Increases in Rainwater Runoff Induced by Land-use Changes

Land uses are not invariable. Deakin University has been one of Australia's fastest-growing universities in the last decade. Among its campuses, an anticipated increase at WP campus will be equivalent to additional 11,000 equivalent full-time student loads in 2020, which will account for 16.2% of the total growth. The campus has been upgrading facilities and constructing infrastructure in response to the increasing demands of teaching and research. Yet, the significant growth of campus infrastructure could lead to environmental impacts, even flooding risk. To analyse the inundation risk, Table 1 lists the top 20 catchments, in which land-use changes over the last decade lead to a significant increase in the rainfall-runoff volume.

It can be observed from the distribution of top catchments that most development was concentrated in the north-western, northern and south-eastern regions between Jul04 and Jan15. Columns 3, 4 and 5 list the change in proportions of raw land, building land and carpark in each catchment over the period, respectively. It is clear that the initial land use did not contain building land within most of these catchments. Also, previous soil types did not contain carpark in half of these catchments.

By Jul15, a marked change was that the percentage of raw land which belonged to Catchment 45 decreased to 37.51% from 100%, chiefly because the percentage of building land had an increase of 5.46%, 36.54% for carparks and 16.70% for roads. As a result, the land-use effect led to a fall of 392.07 m^3 in infiltration volume as shown in Column 6. Within the south-eastern region, the facility construction generated a 237.09 m^3 rainfall-runoff volume over Catchment 11, 173.34 m^3 over Catchment 12, 164.37 m^3 over Catchment 46, 215.10 m^3

TABLE 1. Top 20 increases in the runoff volume due to land-use changes

Catchment	Area	Proportion of raw land (%)	Proportion of building land (%)	Proportion of carpark (%)	Runoff increase	Rank
45	17658 m^2	100.0 → 37.51	0.00 → 5.46	0.00 → 36.54	392.07 m^3	1
51	25192 m^2	99.96 → 67.39	0.04 → 12.69	0.00 → 12.72	298.47 m^3	2
44	28850 m^2	93.79 → 68.54	0.00 → 14.39	0.00 → 3.54	255.44 m^3	3
22	13363 m^2	70.85 → 19.41	0.00 → 0.00	22.66 → 74.10	250.09 m^3	4
11	31583 m^2	100.0 → 79.36	0.00 → 16.91	0.00 → 0.00	237.09 m^3	5
39	19064 m^2	58.38 → 23.93	21.33 → 32.36	5.33 → 21.08	231.98 m^3	6
43	13062 m^2	100.0 → 50.80	0.00 → 18.25	0.00 → 16.56	224.25 m^3	7
47	22198 m^2	100.0 → 69.32	0.00 → 7.41	0.00 → 0.68	215.10 m^3	8
12	24635 m^2	74.41 → 55.07	0.00 → 0.00	21.06 → 40.41	173.34 m^3	9
46	24084 m^2	100.0 → 81.24	0.00 → 8.78	0.00 → 3.45	164.37 m^3	10
41	33363 m^2	72.40 → 58.35	17.62 → 28.10	5.21 → 5.21	153.88 m^3	11
04	11345 m^2	97.19 → 60.64	1.03 → 31.28	1.78 → 3.91	146.06 m^3	12
23	18218 m^2	84.16 → 63.64	0.00 → 0.00	1.69 → 22.21	135.99 m^3	13
31	20845 m^2	91.42 → 75.22	0.00 → 3.58	0.00 → 5.22	112.94 m^3	14
28	14367 m^2	83.97 → 63.55	2.81 → 13.33	8.93 → 10.87	101.15 m^3	15
13	15659 m^2	59.68 → 43.02	0.00 → 6.80	19.19 → 26.75	93.79 m^3	16
53	11010 m^2	70.86 → 47.07	9.44 → 21.32	0.00 → 6.70	91.14 m^3	17
30	9356 m^2	92.75 → 65.75	0.13 → 15.57	0.29 → 7.64	90.55 m^3	18
52	32628 m^2	78.04 → 71.52	0.66 → 4.84	0.00 → 0.00	66.48 m^3	19
49	20456 m^2	67.30 → 57.12	10.17 → 12.58	6.30 → 6.30	65.44 m^3	20

over Catchment 47, 65.44 m^3 over Catchment 49, 224.25 m^3 over Catchment 43 and 255.44 m^3 over Catchment 44. Among them, the proportion of building land increased 18.25 percent for Catchment 43, and the proportion grew 16.91 percent for Catchment 11. Much raw land was used for building construction in the two catchments, which led to 127.18 m^3 and 26.7 m^3 runoff volumes respectively. In addition, 3496.14 m^2 of raw land was converted into building land within Catchment 41, and the path surface area increased by 1192.14 m^2. Corresponding contributions to runoff volumes were respectively 127.18 m^3 and 26.7 m^3. In the south-eastern region of WP campus, a complex of new buildings was completed for improving student accommodation within Catchments 4, 28, 30 and 31, but 450 m^3 total rainwater contributed to drainage volumes, even overland flow. Overall, the expansion of impervious ground surfaces occurred at high elevation, which increased the risk of sewer surcharge around manholes and flood inundation for downstream regions.

5.2. Effects from Land-use Changes under Different Storm Conditions

GIS mapping technologies are used to exhibit the land-use effects on flooding inundation under different storm events. Inundation maps in Figure 5 exhibit the maximum ponding

status induced by Storm TH when considering the previous and current land uses, respectively. The inundation first began with ponding on Nicol Drive North at around 10:30, then flowed eastward to Building *jd*. In addition, the rainwater had surcharged from manholes within Catchment 36 before 11:00. The maximum ponding extents formed after the peak intensity. The 100.26mm rainfall did not lead to extensive flooding within this study area as the rainfall intensity gradually grew and fell with the triangular rainfall distribution. However, both inundation maps shows that the rainwater is ponding in the three main regions, namely, around Building *jd*, between Building *ka* and Lake Drive, and east of Lake Drive.

FIGURE 5. Maximum flooding extents under Storm TH

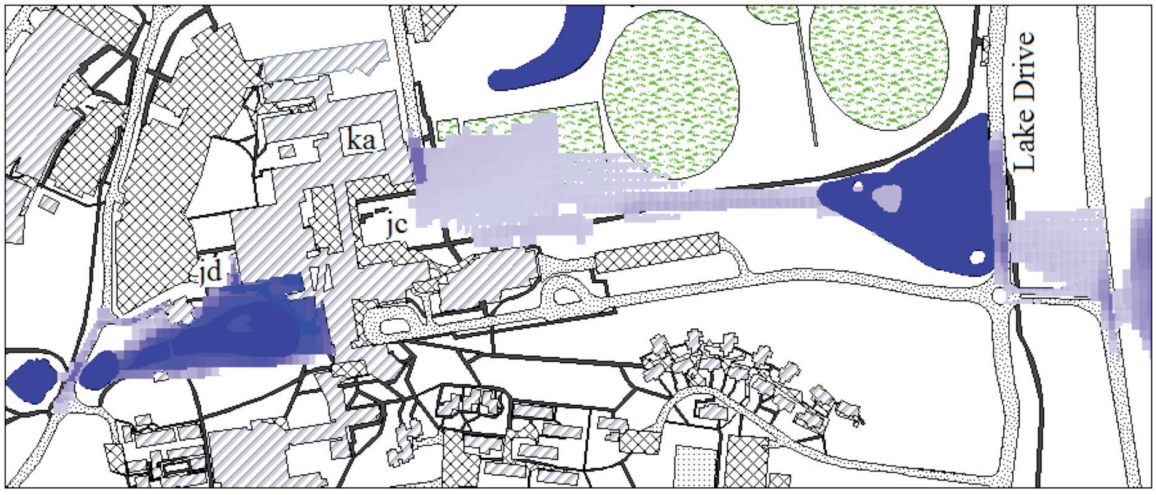

(a) Inundation map when considering previous built environment characteristics

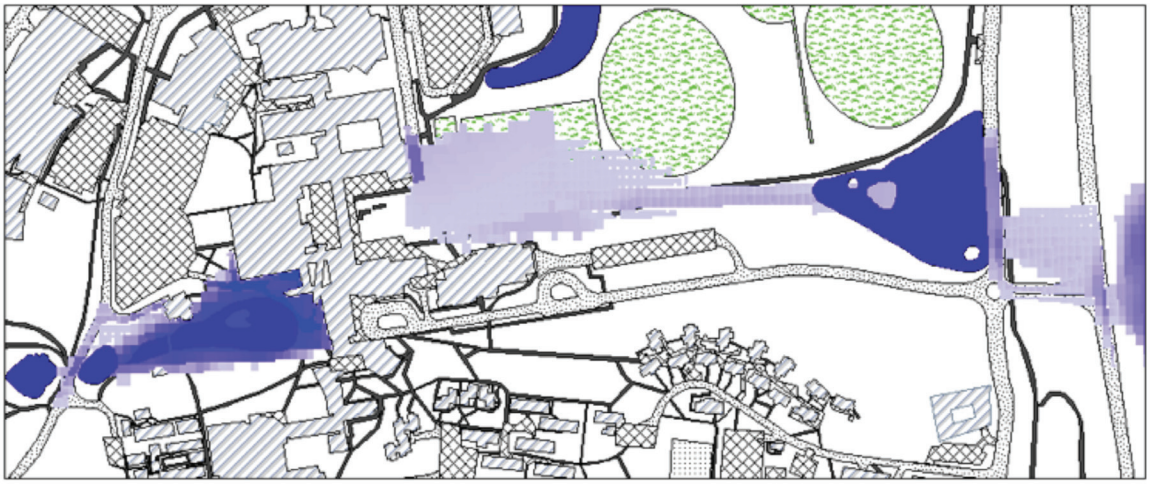

(b) Inundation map when considering current built environment characteristics

Inundation maps in Figure 6 display the maximum ponding extents induced by the Storm HD for different land uses. Storm HD resulted in more extensive flooding as the study area suddenly experienced a two-hour peak intensity at the start. Overflow occurred for manholes within Catchments 1 and 16 because the stormwater volume exceeded the drainage capabilities of the pipe network at around 01:45. The ponding water then appeared to be in

Catchments 15, 36 and 42. These two maps show that the rainwater is ponding in the four main regions, namely, north of Building *oa*, around Building *jd*, between Building *ka* and Lake Drive, and east of Lake Drive.

FIGURE 6. Maximum flooding extents under Storm HD

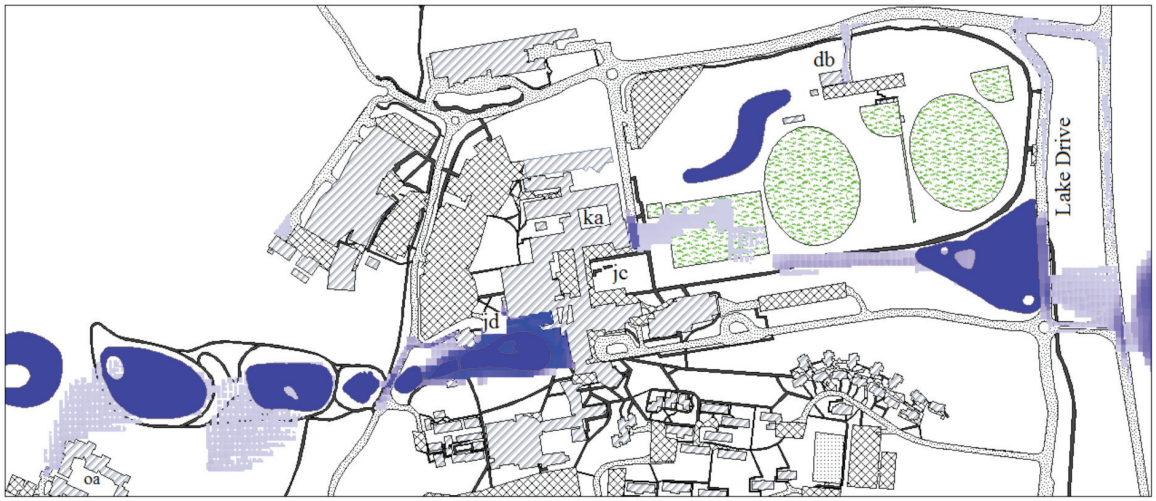

(a) Inundation map when considering previous built environment characteristics

(b) Inundation map when considering current built environment characteristics

For the land uses of Jul04 and Jan15, inundation maps in Figure 7 display the maximum ponding extents resulting from the 100.26mm Storm AB. Initially, flood inundation appeared to be in the low-lying areas of Catchment 42 at around 11:10. Many manholes surcharged after 10 minutes, and floodwater appeared in many regions simultaneously, such as Catchments 1, 8, 11, 15, 16 and 36. The two resulting maps clearly demonstrate the extensive flooding within the range of the WP campus since the 37.34 mm/h peak generated a dramatic change in the rainfall volume. Ponding water was flooding the several main regions, namely west of Building *na*, around Building *jd*, between Building *ka* and Lake Drive, around Building *db* and east of Lake Drive.

FIGURE 7. Maximum flooding extents under Storm AB

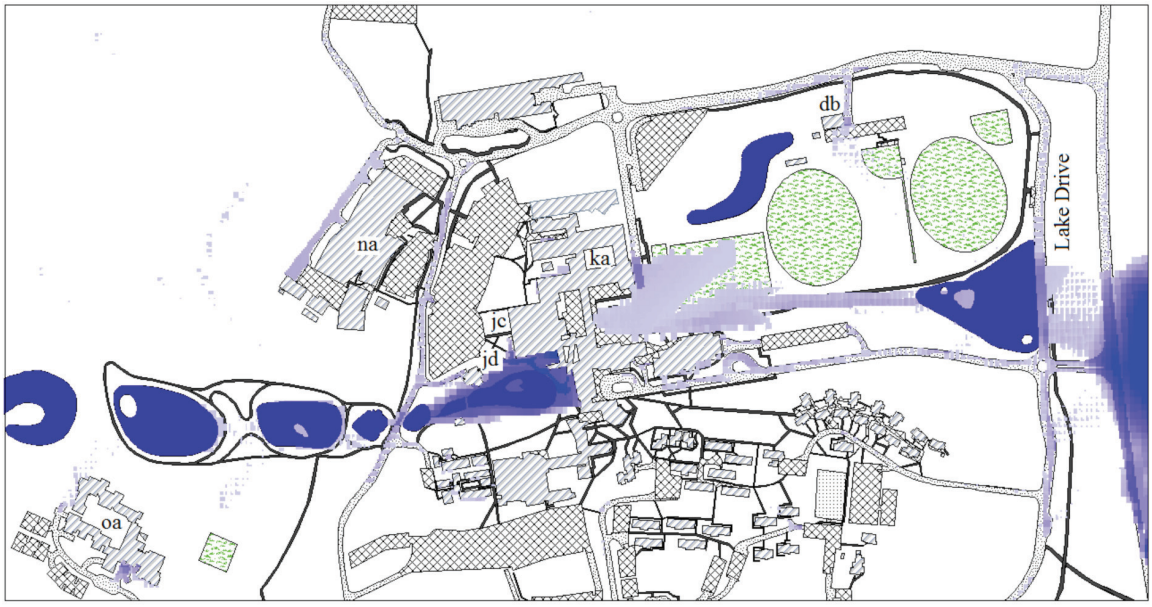

(a) Inundation map when considering previous built environment characteristics

(b) Inundation map when considering current built environment characteristics

To have a better comparison, Table 2 lists the relative indices for measuring the land-use effects on flash floods. The 1D indices aim to present the water levels flooding the whole campus and three flood-prone regions. Corresponding flooding areas were measured as 2D indices. 3D indices are volumes of water discharge and flow to overland. For Storm TH, the maximum water depth across the whole study area was 72.2 cm, which was around Building *jd*, when considering the built environment of Jul04. The total ponding area reached 45,892 m^2. When experiencing the same storm, the deepest water level slightly rose to 76.6cm for the current built

environment. The total ponding area, which increased by around 3260 m^2, covered 49,152 m^2 for the land uses of Jan15. The relatively marked impact on the flood-prone area was that the water level rose by 4.1cm to the east of Lake Drive.

TABLE 2. A comparison of flood-related indices for land-use changes under different rain scenarios

Flood-related indices		Storm TH		Storm HD		Storm AB	
		Jul04	Jan15	Jul04	Jan15	Jul04	Jan15
Maximum Water Depth	Whole study area	72.2 cm	76.6 cm	63.5 cm	67.8 cm	98.2 cm	105.1 cm
	Around Building *jd*	72.2 cm	76.6 cm	63.5 cm	67.8 cm	77.0 cm	81.2 cm
	Between Building *jc* and Lake Drive	29.2 cm	29.7 cm	26.7 cm	30.8 cm	34.8 cm	34.9 cm
	East of Lake Drive	27.5 cm	31.6 cm	27.7 cm	38.5 cm	98.2 cm	105.1 cm
Flooding Area	Whole study area	45892 m^2	49152 m^2	63436 m^2	79224 m^2	84268 m^2	90108 m^2
	Around Building *jd*	12012 m^2	12548 m^2	11688 m^2	11996 m^2	11848 m^2	12140 m^2
	Between Building *jc* and Lake Drive	24376 m^2	26156 m^2	15052 m^2	27460 m^2	29200 m^2	29380 m^2
	East of Lake Drive	9672 m^2	10616 m^2	10320 m^2	13192 m^2	23980 m^2	25184 m^2
Volume	Outlets	70913 m^3	73947 m^3	70834 m^3	73847 m^3	67309 m^3	70496 m^3
	Flow to overland	3920 m^3	4419 m^3	3220 m^3	4069 m^3	6360 m^3	7446 m^3

The second rainfall event, Storm HD, caused the maximum water depth of 63.5 cm, which was also around Building *jd*, considering the previous land uses. The total ponding area reached 63,436 m^2. The current built environment led to an increment of 4.3 cm in the deepest water level after experiencing the same thunder storm. The total flooding area also increased by 15,788 m^2. In particular, the ponding area between Building *jc* and Lake Drive rose by 82.4% from 15,052 m^2. In addition, the impervious areas increased in the north-eastern region and generated 186.3% more rainwater flooding on the road between Buildings *na* and *ni*. Like the first storm scenario, there was no a significant change in the flooding area around Building *jd*.

The high peak intensity of Storm AB can result in extensive flooding within the range of the study area. It caused the maximum water depth of 98.2 cm, which was flooding the eastern boundary, when considering the land uses of Jul04. The total ponding area reached 84,269 m^2. When experiencing the same storm, the deepest water level rose by around 7 cm because the 10-year development replaced much raw land with impervious ground surfaces. There was an increase of 5840 m^2 in the total flooding area. It rose by 7% to 90,108 m^2. The expansion of impervious ground surfaces in the north-eastern region led to the 3550 m^2 rainwater area of ponding on roads. Consequently, it can be concluded that construction-generated impervious ground surfaces tend to affect nearby flood-prone areas. This is because the over-capacity discharge that flows from manholes toward neighbouring areas accumulates on low-lying regions. Overall, urbanised areas could affect the extent of flooding of buildings and roads, and could lead to varying degrees of aggravation of urban flash floods for different storm events.

5.3. A simple control of stormwater runoff

Rainwater storage systems are an effective way of capturing stormwater for non-potable use such as garden watering. As shown in Figure 2, six rainwater storage units are located in Catchments 2, 8, 36, 33 and 6. Each unit has the storage capability of 100,000 litres and is supposed to link with the drainage system for collecting the excess rainwater from the nearby manholes and reducing the stormwater runoff.

For the flood inundation induced by Storm TH, the total flooding area can be reduced by 1872 m^2 from 49125 m^2. Taking the flooding extents around Building *jd* as an example, an 544 m^2 flooding area and a 183 m^3 runoff volume can be avoided through the simple rainwater storage system. The deepest water level can also be decreased by 2 cm. In addition, the total flooding area can be reduced by 1640 m^2 through the runoff control if the study area experiences Storm HD. Flooding areas of around 400 m^2 and 924 m^2 can be avoided within the regions around Building *jd* and east of Lake Drive respectively. The corresponding water levels can be slightly decreased to 66.5 cm and 36.4 cm respectively. However, Storm AB leads to the extensive flooding within the study area. There is no a significant reduction in flooding extents. The total flooding area can only be decreased by around 500 m^2 for the whole study area.

6. CONCLUSIONS

This paper has selected flood inundation as urban built environment research because it has been a growing development challenge for many cities around the world and the most expensive natural hazard in Australia. This research has established a framework of modelling urban flood inundation by examining the effects on flash floods generated by land-use changes. The Geelong WP campus of Deakin University was chosen as a case study. It is assumed that the study area is acted upon by 100.26 mm rainstorm loads with different rainfall distributions. Through GIS-based mapping techniques, resulting maps are proposed for visualising the effects on flood inundation from different features and conditions of the built environment. The results reveal that the construction-induced increase in the impervious ground surfaces tends to affect nearby flooded low-lying areas so that pipe networks are exposed to more drainage pressures. After comparison of inundation maps, most flooding areas are significantly expanded and the maximum flooding depth increases slightly due to large-scale change in the built environment over the last decade. Rainwater storage units may be taken into account for the purposes of flood mitigations.

Additionally, this study is beneficial to urban planning and emergency preparation. It is recommended that the outcomes of this study could be applied to flood assessment measures for urban development and the results could be utilised in government planning to raise awareness of flood hazards. The proposed method could be further extended to the application of flood risk estimation that responds to large-scale urban development and land transformations.

REFERENCES

ABC News. (2011). "Flood costs tipped to top $30b". Australian Broadcasting Corporation. Available at: www.abc.net.au/news/2011-01-18/flood-costs-tipped-to-top-30b/1909700.

American Society of Civil Engineers (1993). *Design and Construction of Urban Stormwater Management Systems*. American Society of Civil Engineers and Water Environment Federation. USA.

BOM (2013). *National Arrangements for Flood Forecasting and Warning*. Bureau of Meteorology (BOM), Commonwealth of Australia. Canberra, Australia.
BOM. (2015a). "Summary of Significant Severe Thunderstorm Events in NSW - 1970/1979". Available at: www.bom.gov.au/nsw/sevwx/7079summ.shtml.
BOM. (2015b). "Climate Data Online". Available at: www.bom.gov.au/climate/data.
BOM. (2015c). "Design rainfall intensity chart". Available at: www.bom.gov.au/hydro/has/cdirswebx/cdirswebx.shtml.
Brody, S., Blessing, R., Sebastian, A. & Bedient, P. (2014). "Examining the impact of land use/land cover characteristics on flood losses". *Journal of Environmental Planning and Management*, Vol. 57, No. 8, pp. 1252-1265.
Brody, S. D., Zahran, S., Highfield, W. E., Grover, H. & Vedlitz, A. (2008). "Identifying the impact of the built environment on flood damage in Texas". *Disasters*, Vol. 32, No. 1, pp. 1-18.
Carbone, D. & Hanson, J. (2013). "Floods: 10 of the deadliest in Australian history". *Australian Geographic*.
Chen, J., Hill, A. A. & Urbano, L. D. (2009). "A GIS-based model for urban flood inundation". *Journal of Hydrology*, Vol. 373, No. 1–2, pp. 184-192.
Chow, V., Maidment, D. & Mays, L. (1988). *Applied Hydrology*. Tata McGraw-Hill Education. USA.
Danish Hydraulic Institute (1999). *MOUSE version 1999 User Manual and Tutorial*. DHI Water & Environment. Hørsholm, Denmark.
Dawod, G. M., Mirza, M. N. & Al-Ghamdi, K. A. (2011). "GIS-based spatial mapping of flash flood hazard in Makkah city, Saudi Arabia". *Journal of Geographic Information System*, Vol. 3, No. 3, pp. 225-231.
Dongquan, Z., Jining, C., Haozheng, W., Qingyuan, T., Shangbing, C. & Zheng, S. (2009). "GIS-based urban rainfall-runoff modeling using an automatic catchment-discretization approach: a case study in Macau". *Environmental Earth Sciences*, Vol. 59, No. 2, pp. 465-472.
Huff, F. A. (1967). "Time distribution of rainfall in heavy storms". *Water Resources Research*, Vol. 3, No. 4, pp. 1007-1019.
Jha, A. K., Bloch, R. & Lamond, J. (2012). *Cities and Flooding: A Guide to Integrated Urban Flood Risk Management for the 21st Century*. World Bank Publications. Washington.
Jiao, P., Xu, D., Wang, S., Yu, Y. & Han, S. (2015). "Improved SCS-CN Method Based on Storage and Depletion of Antecedent Daily Precipitation". *Water Resources Management*, Vol. 29, No. 13, pp. 4753-4765.
Kadam, A., Kale, S., Pande, N., Pawar, N. J. & Sankhua, R. N. (2012). "Identifying potential rainwater harvesting sites of a semi-arid, basaltic region of western India, using SCS-CN method". *Water Resources Management*, Vol. 26, No. 9, pp. 2537-2554.
Kubý, R. & Gustafsson, L. G. (2001). *Application of 3D complex modelling in simulation of extreme discharges in urban areas*. In: Marsalek, J., Watt, E., Zeman, E. & Sieker, H. (eds.) Advances in Urban Stormwater and Agricultural Runoff Source Controls. Netherlands: SpringerLink.
Lee, J. G. & Heaney, J. P. (2003). "Estimation of urban imperviousness and its impacts on storm water systems". *Journal of Water Resources Planning and Management*, Vol. 129, No. 5, pp. 419-426.
Mark, O., Apirumanekul, C., Kamal, M. M. & Praydal, G. (2001). *Modeling of urban flooding in Dhaka city*. Specialty Symposium on Urban Drainage Modeling at the World Water and Environmental Resources Congress, 2001, American Society of Civil Engineers, Orlando, Florida, USA, 333-343.
Mark, O., Weesakul, S., Apirumanekul, C., Aroonnet, S. B. & Djordjević, S. (2004). "Potential and limitations of 1D modelling of urban flooding". *Journal of Hydrology*, Vol. 299, No. 3–4, pp. 284-299.
Middelmann, M. H. (2009). *Review of the Australian Flood Studies Database*. Geoscience Australia. Canberra, Australia.
Mills, N. (2014). "Thunderstorms cause traffic chaos across Geelong". *Geelong Advertiser*.
Mishra, S. K. & Singh, V. P. (2003). *Soil Conservation Service Curve Number (SCS-CN) Methodology*. Kluwer Academic Publishers. Dordrecht.
Nagarajan, N. & Poongothai, S. (2012). "Spatial Mapping of Runoff from a Watershed Using SCS-CN Method with Remote Sensing and GIS". *Journal of Hydrologic Engineering*, Vol. 17, No. 11, pp. 1268-1277.
National Oceanic and Atmospheric Administration (2010). *Flash Flood Early Warning System Reference Guide*. University Corporation for Atmospheric Research. Denver.
Pazwash, H. (2011). *Urban storm water management*. CRC Press Taylor and Francis Group. New York.
Quan, R.-S. (2014). "Rainstorm waterlogging risk assessment in central urban area of Shanghai based on multiple scenario simulation". *Natural Hazards*, Vol. 73, No. 3, pp. 1569-1585.

Ranjan, P., Kazama, S., Sawamoto, M. & Sana, A. (2009). "Global scale evaluation of coastal fresh groundwater resources". *Ocean & Coastal Management*, Vol. 52, No. 3–4, pp. 197-206.

Rossman, L. A. (2010). *Storm Water Management Model User's Manual Version 5.0*. U. S. Environmental Protection Agency,

Sheng, J. & Wilson, J. (2009). "Watershed urbanization and changing flood behavior across the Los Angeles metropolitan region". *Natural Hazards*, Vol. 48, No. 1, pp. 41-57.

Smart, P. & Herbertson, J. G. (1992). *Drainage Design*. Springer US. New York.

Soulis, K. X., Valiantzas, J. D., Dercas, N. & Londra, P. A. (2009). "Investigation of the direct runoff generation mechanism for the analysis of the SCS-CN method applicability to a partial area experimental watershed". *Hydrology and Earth System Sciences*, Vol. 6, No. 5, pp. 605–615.

Thiessen, A. H. (1911). "Precipitation averages for large areas". *Monthly Weather Review*, Vol. 39, No. 7, pp. 1082-1089.

Thomas, J., Prasannakumar, V. & Vineetha, P. (2015). "Suitability of spaceborne digital elevation models of different scales in topographic analysis: an example from Kerala, India". *Environmental Earth Sciences*, Vol. 73, No. 3, pp. 1245-1263.

US Soil Conservation Service (1986). *Urban hydrology for small watersheds*. U. S. Department of Agriculture. Washington, DC.

Wallingford Software (2006). *Infoworks CS, version 7.5, documentation*. Wallingford.

Woodward, D. E., Hawkins, R. H., Jiang, R., Allen T. Hjelmfelt, J., Mullem, J. A. V. & Quan, Q. D. (2003). *Runoff curve number method: examination of the initial abstraction ratio*. World Water & Environmental Resources Congress 2003.

Wu, X., Yu, D., Chen, Z. & Wilby, R. (2012). "An evaluation of the impacts of land surface modification, storm sewer development, and rainfall variation on waterlogging risk in Shanghai". *Natural Hazards*, Vol. 63, No. 2, pp. 305-323.

Yen, B. C. & Chow, V. T. (1980). "Design hyetographs for small drainage structures". *Journal of the Hydraulics Division*, Vol. 106, No. 6, pp. 1055-1076.

Youssef, A., Pradhan, B. & Hassan, A. (2011). "Flash flood risk estimation along the St. Katherine road, southern Sinai, Egypt using GIS based morphometry and satellite imagery". *Environmental Earth Sciences*, Vol. 62, No. 3, pp. 611-623.

Zhang, S. & Pan, B. (2014). "An urban storm-inundation simulation method based on GIS". *Journal of Hydrology*, Vol. 517, pp. 260-268.